ChemComm

Accepted Manuscript

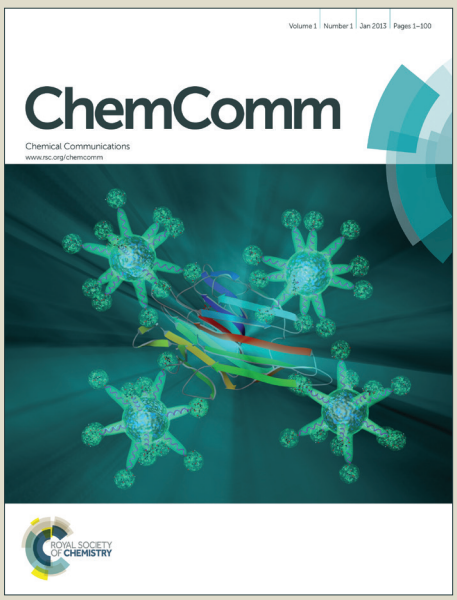

ROYAL SOCIETY OF CHEMISTRY

www.rsc.org/chemcomm

Cite this: DOI: 10.1039/c0xx00000x

www.rsc.org/xxxxxx

ARTICLE TYPE

Electrochemiluminescent swimmers for dynamic enzymatic sensing

Milica Sentic,[a,b,c] Stéphane Arbault,[a,b] Bertrand Goudeau,[a,b] Dragan Manojlovic,[c] Alexander Kuhn,[a,b] Laurent Bouffier,*[a,b] and Neso Sojic*[a,b]

Received (in XXX, XXX) Xth XXXXXXXXX 20XX, Accepted Xth XXXXXXXXX 20XX

DOI: 10.1039/b000000x

An electrochemiluminescent (ECL) swimmer driven by bipolar electrochemistry is reported for enzymatic glucose sensing. The chemo-mechanical motion is induced by localized hydrogen bubble generation. The concomitant oxidation of the luminophore and of the enzymatically-produced NADH leads to ECL emission with a direct glucose-dependant light intensity. We demonstrate herein the local sensing and reporting of glucose in a concentration gradient explored by the ECL swimmer. Such a dynamic sensing approach combines in a synergetic way the wireless propulsion with the enzymatic selectivity using ECL as a readout method at the level of moving objects.

The design of smart systems or machines which are remotely controlled and capable to carry out specific tasks is a fast developing research area. The field is very challenging and explores various applications, especially in healthcare diagnostics, or bio/chemical hazards detection [1–3]. In this context, attention has been focused recently on the motion control of micro- or nano-swimmers that are manipulated or powered by chemicals [4–7] or an external physical input such as electric [8–10] or magnetic fields [4,11,12] or ultrasound [13].

On the other hand, the redox behavior of bipolar electrodes (BEs) is promising for the preparation of complex hybrid materials, surface gradients or analytical applications [14,15]. Bipolar electrochemistry (BPE) offers the possibility to design such swimmers in a very straightforward way as the simple application of an electric field across the solution promotes localized oxygen or hydrogen evolution, leading *in fine* to a motion driven by gas bubble production [10,16,17]. The asymmetric redox activity induced on the BE can also be used to activate other functions such as light emission. This has been demonstrated by developing the concept of electrochemiluminescent swimmers [18,19]. The combination of electrogenerated chemiluminescence (ECL) and BPE has already been reported for sensing purposes with the light emission acting as an analytical readout [20–24]. With that respect, ECL is a very sensitive analytical method that benefits from various advantages including a remarkable signal-to-noise ratio when compared to classic fluorescence monitoring. The fundamental difference is that the luminescence of the luminophore is initiated by an electron transfer (ET) in the case of ECL [25-27] in contrast to photoluminescence, for which the excited state is generated by photon absorption. The ET step takes place at the surface of the electrode, generating reactive species that promote the luminophore to the excited state. Thus, light emission does only occur in the vicinity of the electrode (conductive swimmers herein). The analytical signal is the ECL intensity.

The most common ECL luminophore is the inorganic complex $Ru(bpy)_3^{2+}$ used in combination with tri-*n*-propylamine (TPA) as a sacrificial co-reactant [18]. In this model system, only the ECL luminophore is regenerated during the process, whereas the co-reactant is consumed by the electrochemical reactions. Nevertheless, ECL monitoring of dehydrogenase activity has also been reported because NADH, the reduced form of the co-factor, can equally act as an ECL co-reactant [29-32]. In contrast, the NAD^+ co-factor does not promote ECL and thus the light emission is only electrocatalytically generated in the case of a simultaneous presence of the enzyme and its substrate (*e.g.* glucose), with the enzymatic reaction regenerating the active form of the co-reactant, NADH [30,33].

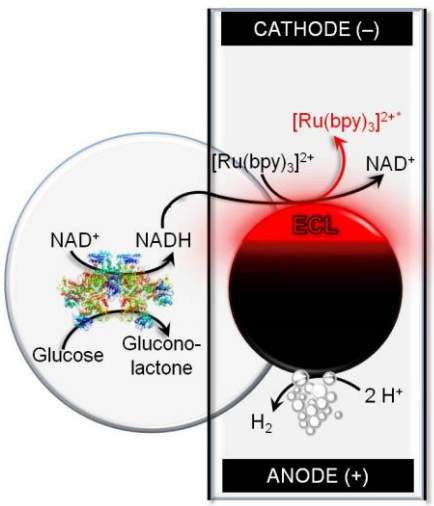

Scheme 1 Illustration of enzyme-driven ECL observed on a bipolar swimmer. Glucose is oxidized by glucose dehydrogenase (GDH) with NAD^+ as a co-factor. The enzymatically-produced NADH behaves as an *in situ* co-reactant for the ECL generation.

Scheme 1 depicts the principle of the swimmer which generates ECL emission only in the presence of glucose. The set-up consists of a glassy carbon (GC) bead positioned in a vertical capillary between two feeder electrodes (Fig. S1) for the application of an adequate electric field [16]. The propulsion mechanism is based on the generation of hydrogen bubbles at the cathodic extremity of the BE which is facing the feeder anode:

$2\ H^+ + 2\ e^- \rightarrow H_2$ (1)

In the absence of glucose, the only reactions occurring at the anodic pole of the swimmer are the oxidation of the ruthenium complex as well as of water according to the following equations:

$Ru(bpy)_3^{2+} \rightarrow Ru(bpy)_3^{3+} + e^-$ (2)

$H_2O \rightarrow ½\ O_2 + 2\ H^+ + 2\ e^-$ (3)

Thus, the oxidation of $Ru(bpy)_3^{2+}$ does not generate any measurable ECL since the enzymatic co-factor remains in the ECL-inactive NAD^+ form. The oxygen bubbles produced at the top of the BE are simply evacuated through the capillary and do not influence the motion. On the other hand, ECL emission occurs when the enzymatic system is turned on in the presence of glucose substrate. Indeed, GDH oxidizes glucose to gluconolactone with the concomitant conversion of NAD^+ to NADH (Scheme 1). In that case, the ET reactions occurring on the BE-beads are the mono-electronic oxidation of $Ru(bpy)_3^{2+}$ and of NADH to the corresponding cationic radical, which can promote the whole sequence of reactions leading to ECL emission:

$Ru(bpy)_3^{2+} \rightarrow Ru(bpy)_3^{3+} + e^-$ (2)

$NADH \rightarrow NADH^{\bullet+} + e^-$ (4)

$NADH^{\bullet+} \rightarrow NAD^{\bullet} + H^+$ (5)

$Ru(bpy)_3^{3+} + NAD^{\bullet} \rightarrow [Ru(bpy)_3^{2+}]^* + NAD^+$ (6)

$[Ru(bpy)_3^{2+}]^* \rightarrow Ru(bpy)_3^{2+} + h\nu$ (7)

It is worth mentioning that the initial state of the co-factor (*i.e.* NAD^+) is regenerated at the end of the ECL mechanism. It is thus available to react again with the enzyme and the process is catalytic. Therefore, a difference in glucose concentration should be easy to distinguish by measuring the ECL intensity.

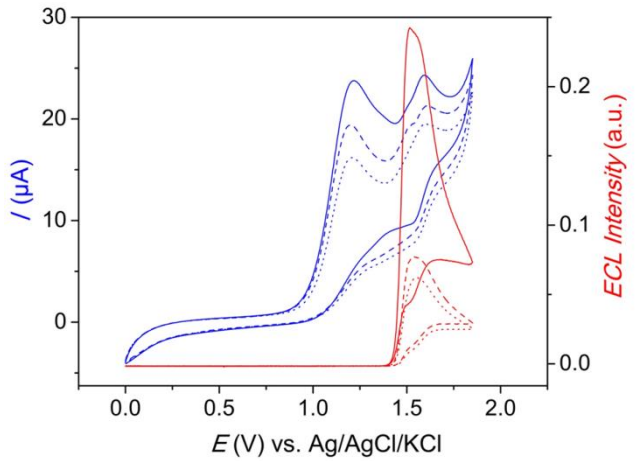

Fig. 1 Cyclic voltammograms (blue lines) and ECL signals (red lines) of 1.5 mM $Ru(bpy)_3^{2+}$ in the presence of 10 $U.mL^{-1}$ GDH, 10 mM NAD^+ and various glucose concentrations (5 mM, dotted lines; 10 mM, dashed lines and 40 mM, solid lines) in 100 mM PBS solution (pH 7.4). A GC electrode (same material as the swimmer) was used to record both CV and ECL. Scan rate 0.05 $V.s^{-1}$.

Fig. 1 gathers the cyclic voltammograms (CV, blue lines) and the corresponding ECL intensity (red lines) of a series of solutions containing various amounts of glucose. These data were recorded 30 minutes after mixing GDH, NAD^+ and glucose in 100 mM PBS solution (pH 7.4). NADH oxidation occurs first and the ET is irreversible with an anodic peak centered at ~ 1.2 V *vs.* Ag/AgCl. The oxidation of $Ru(bpy)_3^{2+}$ takes place at slightly more anodic potential (E°' ~ 1.55 V *vs.* Ag/AgCl). A careful examination of the ECL signal recorded during the CV shows that the emission perfectly matches with the potential region where $Ru(bpy)_3^{2+}$ is oxidized. The ECL mechanism clearly involves a reaction between both intermediate species formed by the oxidation of NADH and $Ru(bpy)_3^{2+}$.

Increasing the glucose concentration from 5 to 40 mM results in raising the level of NADH in solution. This increase can be monitored by measuring the ECL intensity. Indeed, the ECL intensity is dependent on the initial glucose content.

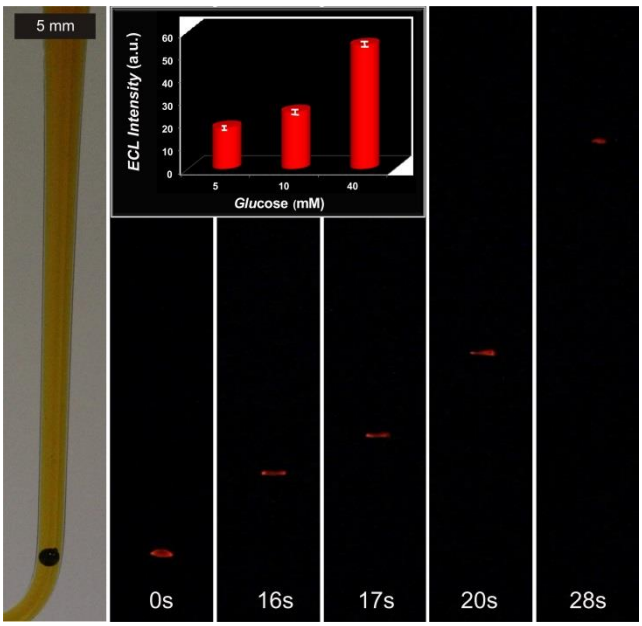

Fig. 2 ECL sensing and reporting of glucose concentration during the swimmer motion. Series of optical images showing a GC bead emitting ECL at different times during its motion. The GC bead is positioned in a U-shaped cell, filled with 100 mM PBS solution (pH 7.4) containing 10 $U.mL^{-1}$ GDH, 1.5 mM $Ru(bpy)_3^{2+}$, 10 mM NAD^+, 40 mM glucose and a few drops of surfactant. Applied electric field: 23 $V.cm^{-1}$. The left image is recorded under white light whereas the others images were taken in the dark. Inset: Plot showing the dependence of the ECL signal on the glucose concentration.

Fig. 2 shows the experimental configuration when the BE acts as an ECL swimmer. The application of a sufficient electric field (Fig. S2) drives the asymmetric electrochemical reactions on both poles of the bead. The production of H_2 bubbles below the bead (cathodic pole) induces its motion. On the anodic pole, ECL might be generated. The ECL emission is clearly visible by the naked eye in the presence of glucose and the position of the bead could be recorded by using a commercial camera during the rise of the swimmer (Video S1). A negative control experiment recorded without any glucose in solution does not produce any measurable light emission. Such an approach, also called photoscopy is becoming increasingly popular as it is easy and cheap to perform [34,35]. The ECL intensity monitored at the top of the bead is proportional to the glucose concentration as reported in the inset of Fig. 2. One can note that the shape of the ECL emission evolves with time as reported previously [18]. Nevertheless, the overall intensity was analysed (Image J software) and this reveals a direct relationship between glucose concentration and the relative luminescence signal. Indeed, the

ECL intensity reflects the local NADH concentration which is directly related to the enzymatic activity, and thus to the concentration of the substrate. Therefore, in the present case, the ECL swimmer is a dynamic reporter of the local concentration of glucose. The levitation of the swimmer stops when switching off the electric field. After sinking to the bottom of the capillary, the ECL swimmer can be activated again by reapplying the electric field.

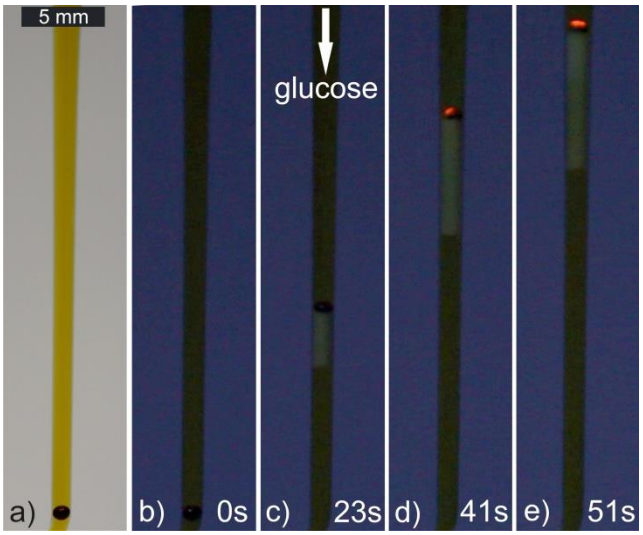

Fig. 3 Images illustrating the switching-on of ECL during the swimmer motion in a vertical glucose concentration gradient. The U-shaped cell is filled with 100 mM PBS solution (pH 7.4) containing 2.5 mM $Ru(bpy)_3^{2+}$, 10 $U.mL^{-1}$ GDH and 10 mM NAD^+. The same solution but containing in addition 40 mM glucose was introduced at the top of the capillary. The established vertical concentration gradient is revealed by ECL. The left image (a) is recorded under ambient light before applying the electric field. The other images (b-e) were taken after the application of the electric field (23 $V.cm^{-1}$) under low external white light illumination in order to image the bead motion during the ECL sensing of glucose.

Due to the dependence of ECL intensity on glucose concentration, this approach is also suitable to monitor the spatial distribution of variations in glucose concentration. In other words, if the swimmer moves in inhomogeneous media, then ECL will only be activated at locations where the analyte is present. To demonstrate this ability to switch on the ECL, the GC bead was positioned in a capillary filled with a PBS solution containing the ECL reporter, the enzyme and the co-factor. Another solution containing glucose in addition was introduced dropwise at the very top of the capillary (arrow on Fig. 3c). This generates a vertical concentration gradient where the higher amount of glucose and thus of NADH is localized at the top part. Fig. 3 gathers a series of relevant snapshots extracted from Video S2. As previously, the GC bead is initially positioned at the bottom of the capillary as observed under white light (Fig. 3a). As soon as a sufficient electric field is turned on, proton reduction is promoted underneath the BE. This is clearly visible in Fig. 3c where a train of bubbles can be seen below the bead which is moving up. As soon as the GC bead reaches the location where glucose is present in solution, ECL is switched on, thus demonstrating the possibility of dynamic glucose detection (Fig. 3d). As the swimmer is moving towards a region of higher glucose concentration (top of the capillary), its ECL intensity increases (Fig. 3e). This experiment demonstrates the combined local enzymatic sensing and ECL reporting of an analyte in space and time.

Conclusions

The design of dynamic systems driven by BPE is used here for the first time to perform an analytical task and monitor the glucose concentration in a PBS solution. The substrate is consumed by glucose dehydrogenase with the concomitant conversion of NAD^+ to NADH, the latter promoting $Ru(bpy)_3^{2+}$ ECL *via* the classic co-reactant pathway. This contribution demonstrates that the development of such ECL swimmers could lead to bioanalytical applications allowing the study of locally inhomogeneous samples. The approach broadens significantly the potentialities of BPE in analytical sciences [20–24,36]. In that context, combining BPE and ECL offers a unique analytical platform based on the design of smart dynamic systems for a straightforward visual readout.

Acknowledgements

We acknowledge financial support from the Ministry of Science and Technological Development (Republic of Serbia) and from the French Foreign Ministry (Bourse d'Excellence Eiffel).

Notes and references

[a] *Univ. Bordeaux, ISM, UMR 5255, F-33400 Talence, France. Fax: +33 54000 2717; Tel: +33 54000 2496; E-mails: Laurent.Bouffier@enscbp.fr; Neso.Sojic@enscbp.fr*
[b] *CNRS, ISM, UMR 5255, F-33400 Talence, France.*
[c] *Faculty of Chemistry, University of Belgrade, P.O. Box 158, 11001 Belgrade, Serbia*

† Electronic Supplementary Information (ESI) available: Experimental setup. Electrochemical and ECL characterisation. Videos of the swimmers. See DOI: 10.1039/b000000x/

1 M. Guix, C. C. Mayorga-Martinez, and A. Merkoçi, *Chem. Rev.*, DOI: 10.1021/cr400273r.
2 M. Guix, J. Orozco, M. García, W. Gao, S. Sattayasamitsathit, A. Merkoçi, A. Escarpa and J. Wang, *ACS Nano*, 2012, **6**, 4445.
3 J. Orozco, G. Cheng, D. Vilela, S. Sattayasamitsathit, R. Vazquez-Duhalt, G. Valdés-Ramírez, O. S. Pak, A. Escarpa, C. Kan and J. Wang, *Angew. Chem. Int. Ed.*, 2013, **52**, 13276.
4 T. R. Kline, W. F. Paxton, T. E. Mallouk and A. Sen, *Angew. Chem. Int. Ed.*, 2005, **44**, 744.
5 S. Fournier-Bidoz, A. C. Arsenault, I. Manners and G. A. Ozin, *Chem. Commun.*, 2005, 441.
6 Z. Fattah, G. Loget, V. Lapeyre, P. Garrigue, C. Warakulwit, J. Limtrakul, L. Bouffier and A. Kuhn, *Electrochim. Acta*, 2011, **56**, 10562
7 W. Gao, A. Uygun and J. Wang, *J. Am. Chem. Soc.*, 2012, **134**, 897.
8 S. T. Chang, V. N. Paunov, D. N. Petsev and O. D. Velev, *Nat. Mater.*, 2007, **6**, 235.
9 M. Pumera, *Nanoscale*, 2010, **2**, 1643.
10 G. Loget and A. Kuhn, *Nat. Commun.*, 2011, **2**, 535.
11 A. Ghosh and P. Fischer, *Nano Lett.*, 2009, **9**, 2243.
12 K. E. Peyer, S. Tottori, F. Qiu, L. Zhang and B. J. Nelson, *Chem. Eur. J.*, 2013, **19**, 28.
13 W. Wang, L. A. Castro, M. Hoyos and T. E. Mallouk, *ACS Nano*, 2012, **6**, 6122.
14 S. E. Fosdick, K. N. Knust, K. Scida and R. M. Crooks, *Angew. Chem. Int. Ed.* 2013, **52,** 10438.
15 G. Loget, D. Zigah, L. Bouffier, N. Sojic and A. Kuhn, *Acc. Chem. Res.* 2013, **46**, 2513.
16 G. Loget and A. Kuhn, *Lab Chip*, 2012, **12**, 1967.
17 L. Bouffier and A. Kuhn, *Nanoscale*, 2013, **5**, 1305.

18 M. Sentic, G. Loget, D. Manojlovic, A. Kuhn and N. Sojic, *Angew. Chem. Int. Ed.*, 2012, **51**, 11284.
19 L. Bouffier, D. Zigah, C. Adam, M. Sentic, Z. Fattah, D. Manojlovic, A. Kuhn and N. Sojic, *ChemElectroChem*, 2014, **1**, 95.
20 K.-F. Chow, F. Mavré and R. M. Crooks, *J. Am. Chem. Soc.* 2008, **130**, 7544.
21 K.-F. Chow, F. Mavré, J. A. Crooks, B.-Y. Chang and R. M. Crooks, *J. Am. Chem. Soc.* 2009, **131**, 8364.
22 X. Zhang, C. Chen, J. Li, L. Zhang and E. Wang, *Anal. Chem.* 2013, **85**, 5335.
23 M.-S. Wu, D.-J. Yuan, J.-J. Xu and H.-Y. Chen, *Chem. Sci.*, 2013, **4**, 1182.
24 T. Wang, S. Fan, R. Erdmann and C Shannon, *Langmuir*, 2013, **29**, 16040.
25 N. Tokel and A. J. Bard, *J. Am. Chem. Soc.* 1972, **94**, 2862.
26 A. W. Knight and G. M. Greenway, *Analyst*, 1994, **119**, 879.
27 M. M. Richter, *Chem. Rev.*, 2004, **104**, 3003.
28 I. Rubinstein and A. J. Bard, *J. Am. Chem. Soc.* 1981, **103**, 512.
29 T. M. Downey and T. A. Nieman, *Anal. Chem.*, 1992, **64**, 261.
30 A. F. Martin and T. A. Nieman, *Anal. Chim. Acta*, 1993, **281**, 475.
31 F. Jameison, R. I. Sanchez, L. Dong, J. K. Leland, D. Yost and M. T. Martin, *Anal. Chem.*, 1996, **68**, 1298.
32 M. Milutinovic, S. Sallard, D. Manojlovic, N. Mano and N. Sojic, *Bioelectrochem.*, 2011, **82**, 63.
33 X.-M. Chen, B.-Y. Su, X.-H. Song, Q.-A. Chen, X. Chen and X.-R. Wang, *Tr. Anal. Chem.*, 2011, **30**, 665.
34 T. Schwaebel, S. Menning and U. H. F. Bunz, *Chem. Sci.*, 2014, **5**, 1422.
35 E. H. Doeven, G. J. Barbante, E. Kerr, C. F. Hogan, J. A. Endle and P. S. Francis, *Anal. Chem.*, 2014, **86**, 2727.
36 L. Bouffier, T. Doneux, B. Goudeau and A. Kuhn, *Anal. Chem.*, 2014, **86**, 3708.